

# ANALYTICAL AND NUMERICAL APPROACHES FOR THE COMPUTATION OF AEROELASTIC SENSITIVITIES USING THE DIRECT AND ADJOINT METHODS

Lukas Scheucher

Stanford University

October 2016 - June 2017



Stanford  
University

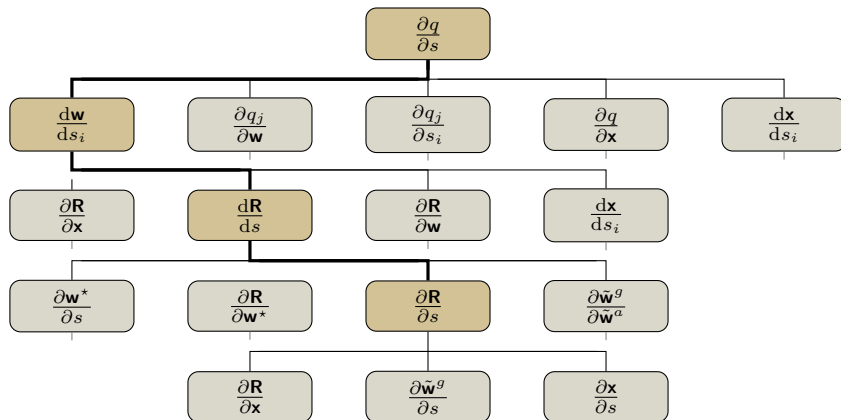
# OVERVIEW

- 1 INTRODUCTION
- 2 AERODYNAMIC OPTIMIZATION
- 3 SENSITIVITY ANALYSIS
- 4 NUMERICAL FRAMEWORK
- 5 NUMERICAL RESULTS
- 6 VERIFICATION

# OUTLINE FOR SECTION 1

- 1 INTRODUCTION
- 2 AERODYNAMIC OPTIMIZATION
- 3 SENSITIVITY ANALYSIS
- 4 NUMERICAL FRAMEWORK
- 5 NUMERICAL RESULTS
- 6 VERIFICATION

AAA



# MOTIVATION

## -> WHY SENSITIVITY ANALYSIS?

- Requirements on CFD
  - Complex flows (transonic, turbulent ...) and high Reynolds numbers
  - Well-resolved boundary layers and flow features
  - Steady/unsteady flows
  - Numerical accuracy, solver robustness and short turn-around time
  - Moderate to highly complex geometries
- Requirements on design and optimization
  - Automatic framework
  - Efficient optimization algorithms
  - Large number of design variables
  - Multi-point design and multi-disciplinary design optimization
  - Geometrical/engineering constraints

# MOTIVATION

## -> WHY EMBEDDED FRAMEWORK?

- Requirements on CFD
  - **Complex flows (transonic, turbulent ...) and high Reynolds numbers**
  - Well-resolved boundary layers and flow features
  - Steady/unsteady flows
  - Numerical accuracy, solver robustness and short turn-around time
  - **Moderate to highly complex geometries**
- Requirements on design and optimization
  - Automatic framework
  - Efficient optimization algorithms
  - Large number of design variables
  - Multi-point design and multi-disciplinary design optimization
  - Geometrical/engineering constraints

→ **Embedded framework**

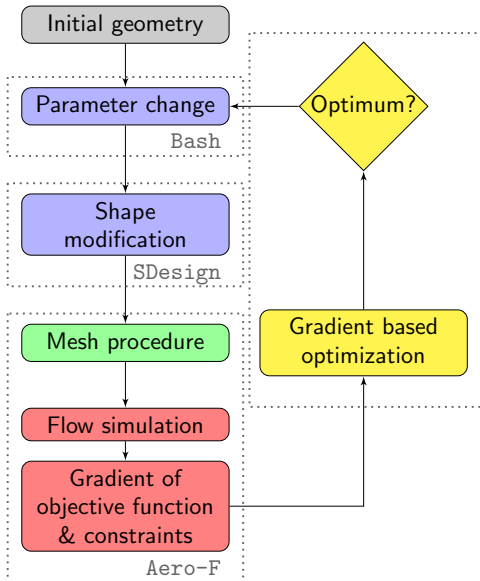
# MOTIVATION

## -> WHY ANALYTIC APPROACH?

- Requirements on CFD
  - Complex flows (transonic, turbulent ...) and high Reynolds numbers
  - Well-resolved boundary layers and flow features
  - Steady/unsteady flows
  - **Numerical accuracy, solver robustness and short turn-around time**
  - Moderate to highly complex geometries
- Requirements on design and optimization
  - Automatic framework
  - Efficient optimization algorithms
  - **Large number of design variables**
  - Multi-point design and multi-disciplinary design optimization
  - Geometrical/engineering constraints

→ **Analytic Sensitivities**

# AERODYNAMIC SHAPE OPTIMIZATION



## GRADIENT BASED OPTIMIZATION

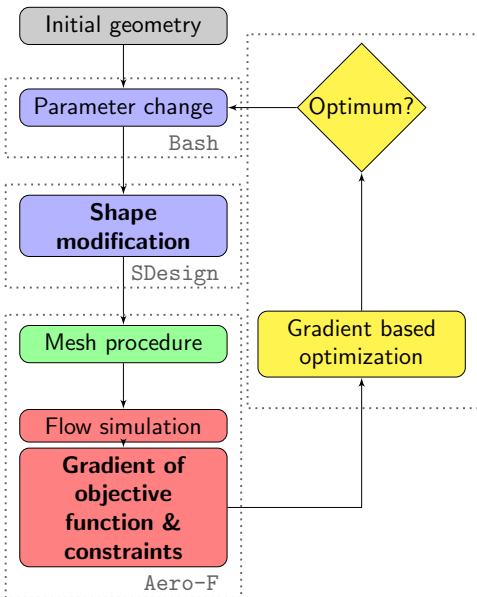
- Requires objective function and constraints
- Gradient of objective function and constraints

## HOW TO COMPUTE THE GRADIENT

- Finite difference
- Direct approach
- Adjoint approach



# AERODYNAMIC SHAPE OPTIMIZATION



## GRADIENT BASED OPTIMIZATION

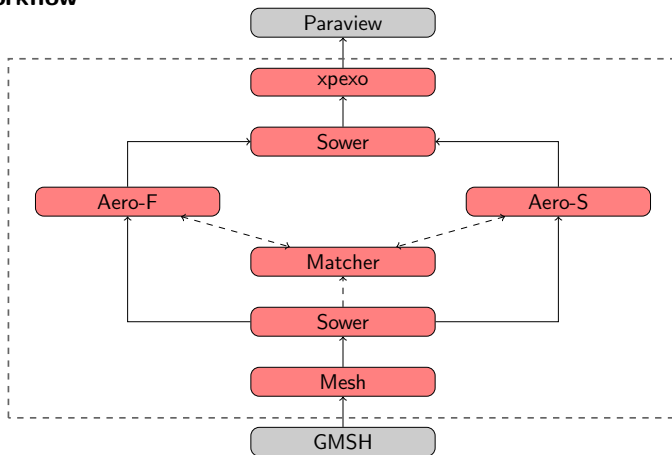
- Requires objective function and constraints
- Gradient of objective function and constraints

## HOW TO COMPUTE THE GRADIENT

- Finite difference
- **Direct approach**
- Adjoint approach

# THE AERO-SUITE<sup>12</sup>

## Aero - workflow

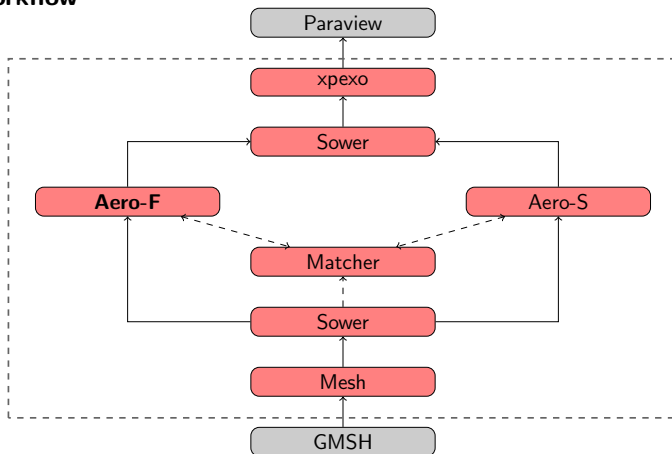


<sup>1</sup>Aerof.

<sup>2</sup>Aeros.

# THE AERO-SUITE<sup>12</sup>

## Aero - workflow



<sup>1</sup>Aerof.

<sup>2</sup>Aeros.

## OUTLINE FOR SECTION 2

- 1 INTRODUCTION
- 2 AERODYNAMIC OPTIMIZATION**
- 3 SENSITIVITY ANALYSIS
- 4 NUMERICAL FRAMEWORK
- 5 NUMERICAL RESULTS
- 6 VERIFICATION

# PDE-CONSTRAINED OPTIMIZATION

- PDE-constrained optimization for steady problems

$$\begin{array}{ll}\text{minimize}_{\mathbf{w} \in \mathbb{R}^{N_{\mathbf{w}}}, s \in \mathbb{R}^{N_s}} & q(\mathbf{w}, s) \\ \text{subject to} & \mathbf{R}(\mathbf{w}, s) = 0 \\ & \mathbf{c}(\mathbf{w}, s) \leq 0\end{array}$$

- Nested approach

$$\begin{array}{ll}\text{minimize}_{\boldsymbol{\mu} \in \mathbb{R}^{N_{\boldsymbol{\mu}}}} & q(\mathbf{w}(s), s) \\ \text{subject to} & \mathbf{c}(\mathbf{w}(s), s) \leq 0.\end{array}$$

# PDE-CONSTRAINED OPTIMIZATION

- PDE-constrained optimization for steady problems

$$\begin{array}{ll}\text{minimize}_{\mathbf{w} \in \mathbb{R}^{N_{\mathbf{w}}}, s \in \mathbb{R}^{N_s}} & q(\mathbf{w}, s \rightarrow \text{e.g. Lift-Drag ratio} \\ \text{subject to} & \mathbf{R}(\mathbf{w}, s) = 0 \\ & \mathbf{c}(\mathbf{w}, s) \leq 0\end{array}$$

- Nested approach

$$\begin{array}{ll}\text{minimize}_{\boldsymbol{\mu} \in \mathbb{R}^{N_{\boldsymbol{\mu}}}} & q(\mathbf{w}(s), s) \\ \text{subject to} & \mathbf{c}(\mathbf{w}(s), s) \leq 0.\end{array}$$

# PDE-CONSTRAINED OPTIMIZATION

- PDE-constrained optimization for steady problems

$$\begin{array}{ll} \underset{\mathbf{w} \in \mathbb{R}^{N_{\mathbf{w}}}, s \in \mathbb{R}^{N_s}}{\text{minimize}} & q(\mathbf{w}, s) \rightarrow \text{e.g. Lift-Drag ratio} \\ \text{subject to} & \mathbf{R}(\mathbf{w}, s) = 0 \rightarrow \text{e.g. geometry of engine mount} \\ & \mathbf{c}(\mathbf{w}, s) \leq 0 \end{array}$$

- Nested approach

$$\begin{array}{ll} \underset{\boldsymbol{\mu} \in \mathbb{R}^{N_{\boldsymbol{\mu}}}}{\text{minimize}} & q(\mathbf{w}(s), s) \\ \text{subject to} & \mathbf{c}(\mathbf{w}(s), s) \leq 0. \end{array}$$

# PDE-CONSTRAINED OPTIMIZATION

- PDE-constrained optimization for steady problems

$$\begin{array}{ll} \underset{\mathbf{w} \in \mathbb{R}^{N_{\mathbf{w}}}, s \in \mathbb{R}^{N_s}}{\text{minimize}} & q(\mathbf{w}, s) \rightarrow \text{e.g. Lift-Drag ratio} \\ \text{subject to} & \mathbf{R}(\mathbf{w}, s) = 0 \rightarrow \text{e.g. geometry of engine mount} \\ & \mathbf{c}(\mathbf{w}, s) \leq 0 \rightarrow \text{e.g. Lift-Drag ratio} \end{array}$$

- Nested approach

$$\begin{array}{ll} \underset{\boldsymbol{\mu} \in \mathbb{R}^{N_{\boldsymbol{\mu}}}}{\text{minimize}} & q(\mathbf{w}(s), s) \\ \text{subject to} & \mathbf{c}(\mathbf{w}(s), s) \leq 0. \end{array}$$



## OUTLINE FOR SECTION 3

- 1 INTRODUCTION
- 2 AERODYNAMIC OPTIMIZATION
- 3 SENSITIVITY ANALYSIS**
- 4 NUMERICAL FRAMEWORK
- 5 NUMERICAL RESULTS
- 6 VERIFICATION

# COMPUTATION OF THE GRADIENT

## • Gradients of the objective function

$$\begin{aligned}
 \left. \frac{dq_j}{ds_i} \right|_{w_0} = & \underbrace{\left. \frac{\partial q_j}{\partial s_i} \right|_{w_0}}_{\text{directly derived from the definition of } q} + \underbrace{\left. \frac{\partial q_j}{\partial \mathbf{w}} \right|_{w_0}}_{\text{derived analytically or by FD}} \underbrace{\left. \frac{d\mathbf{w}}{ds_i} \right|_{w_0}}_{\text{derived from dynamic fluid equilibrium}} + \\
 & \underbrace{\left. \frac{\partial q}{\partial \mathbf{x}} \right|_{w_0}}_{\text{derived analytically or by FD}} \underbrace{\left. \frac{\partial \mathbf{x}}{\partial s_i} \right|_{w_0}}_{\text{derived from SDESIGN}} \\
 & \underbrace{\hspace{10em}}_{=0 \text{ for Embedded}}
 \end{aligned}$$

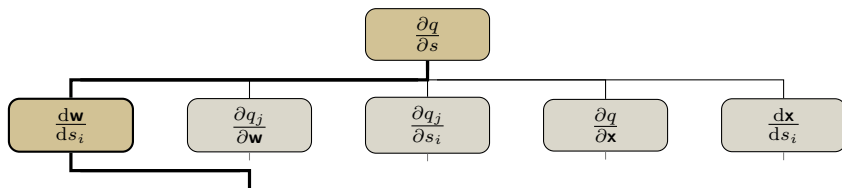
# COMPUTATION OF THE GRADIENT

## Gradients of the objective function

$$\begin{aligned}
 \left. \frac{dq_j}{ds_i} \right|_{w_0} = & \underbrace{\left. \frac{\partial q_j}{\partial s_i} \right|_{w_0}}_{\text{directly derived from the definition of } q} + \underbrace{\left. \frac{\partial q_j}{\partial \mathbf{w}} \right|_{w_0}}_{\text{derived analytically or by FD}} \underbrace{\left. \frac{d\mathbf{w}}{ds_i} \right|_{w_0}}_{\text{derived from dynamic fluid equilibrium}} + \\
 & \underbrace{\left. \frac{\partial q}{\partial \mathbf{x}} \right|_{w_0}}_{\text{derived analytically or by FD}} \underbrace{\left. \frac{\partial \mathbf{x}}{\partial s_i} \right|_{w_0}}_{\text{derived from SDESIGN}} \\
 & \underbrace{\hspace{10em}}_{=0 \text{ for Embedded}}
 \end{aligned}$$

→ **We only look into this term!**

## AAA



## DERIVATION OF $\frac{\partial \mathbf{w}}{\partial s}$

- Consider the fluid equations at equilibrium

$$\cancel{\frac{\partial \bar{\mathbf{w}}_i}{\partial t}} + \underbrace{\sum_{j \in \kappa(i)} \phi_{ij}(\mathbf{w}_{ij}, \mathbf{w}_{ji}, \nu_{ij})}_{\mathbf{R}^i} - \underbrace{\sum_{T_i \in \lambda(i)} \int_{T_j} \mathbb{K} \nabla \mathbf{w} \nabla \phi_j dx}_{\mathbf{R}^v} = \mathbf{0}$$

$\underbrace{\hspace{15em}}_{\mathbf{R}}$

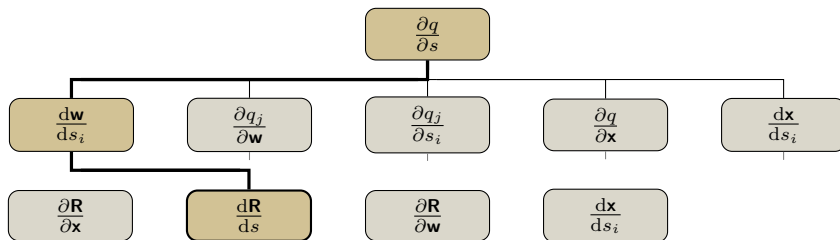
- Therefore

$$\frac{d\mathbf{R}}{ds_i} = \mathbf{0} = \frac{\partial \mathbf{R}}{\partial s_i} + \frac{\partial \mathbf{R}}{\partial \mathbf{w}} \frac{d\mathbf{w}}{ds_i} + \frac{\partial \mathbf{R}}{\partial \mathbf{x}} \frac{d\mathbf{x}}{ds_i}$$

- Which leads to

$$\frac{\partial \mathbf{R}}{\partial \mathbf{w}} \frac{d\mathbf{w}}{ds_i} = -\frac{d\mathbf{R}}{ds_i} - \frac{\partial \mathbf{R}}{\partial \mathbf{x}} \frac{d\mathbf{x}}{ds_i}$$

## AAA



- The final system can be written as

# DERIVATION OF $\frac{\partial \mathbf{R}}{\partial \mathbf{w}}$

$$\frac{\partial \mathbf{R}_{ij}^{c,i}}{\partial \mathbf{w}_k} = \frac{\partial \mathbf{R}_{ij}^{c,i}}{\partial \tilde{\mathbf{w}}_{ij}^*} \frac{\partial \tilde{\mathbf{w}}_{ij}^*}{\partial \tilde{\mathbf{w}}_k} \frac{\partial \tilde{\mathbf{w}}_k}{\partial \mathbf{w}_k} + \frac{\partial \mathbf{R}_{ij}^{c,i}}{\partial \tilde{\mathbf{w}}_{ij}} \frac{\partial \tilde{\mathbf{w}}_{ij}}{\partial \tilde{\mathbf{w}}_k} \frac{\partial \tilde{\mathbf{w}}_k}{\partial \mathbf{w}_k} + \underbrace{\frac{\partial \mathbf{R}_{ij}^{c,i}}{\partial \mathbf{x}} \frac{\partial \mathbf{x}}{\partial n_{ij}}}_{=0 \text{ for embedded}}$$

- Analytical Jacobian of the (Roe's) centering flux
- Analytical derivative of the solution of the 1D half-Riemann problem
- Analytical derivative of the MUSCL reconstruction and limitation



# DERIVATION OF $\frac{\partial \mathbf{R}}{\partial \mathbf{w}}$

$$\frac{\partial \mathbf{R}_{ij}^{c,i}}{\partial \mathbf{w}_k} = \frac{\partial \mathbf{R}_{ij}^{c,i}}{\partial \tilde{\mathbf{w}}_{ij}^*} \frac{\partial \tilde{\mathbf{w}}_{ij}^*}{\partial \tilde{\mathbf{w}}_k} \frac{\partial \tilde{\mathbf{w}}_k}{\partial \mathbf{w}_k} + \frac{\partial \mathbf{R}_{ij}^{c,i}}{\partial \tilde{\mathbf{w}}_{ij}} \frac{\partial \tilde{\mathbf{w}}_{ij}}{\partial \tilde{\mathbf{w}}_k} \frac{\partial \tilde{\mathbf{w}}_k}{\partial \mathbf{w}_k} + \underbrace{\frac{\partial \mathbf{R}_{ij}^{c,i}}{\partial \mathbf{x}} \frac{\partial \mathbf{x}}{\partial n_{ij}}}_{=0 \text{ for embedded}}$$

- Analytical Jacobian of the (Roe's) centering flux
- Analytical derivative of the solution of the 1D half-Riemann problem
- Analytical derivative of the MUSCL reconstruction and limitation

→ We don't go into any more detail here!

The interface component is determined by the structure. Having obtained this one, the interior component can be computed by solving an auxiliary, fictitious Dirichlet problem:

$$\frac{d\dot{\mathbf{x}}_{\Omega}}{ds_i} = - \left[ \bar{\mathbf{K}}_{\Omega\Omega}^{-1} \bar{\mathbf{K}}_{\Omega\Gamma} \right] \frac{d\mathbf{x}_{\Gamma}}{ds_i}$$

$$\frac{dq_j}{ds_i} \Big|_{\mathbf{w}_0} = - \frac{dq_j}{d\mathbf{w}} \Big|_{\mathbf{w}_0} \left[ \frac{\partial \mathbf{R}}{\partial \mathbf{w}} \Big|_{\mathbf{w}_0} \right]^{-1} \left( \frac{\partial \mathbf{R}}{\partial s_i} \Big|_{\mathbf{w}_0} + \left[ \alpha \frac{\partial \mathbf{R}}{\partial \dot{\mathbf{x}}_{\Omega}} \Big|_{\mathbf{w}_0} \frac{\partial \mathbf{R}}{\partial \dot{\mathbf{x}}_{\Gamma}} \Big|_{\mathbf{w}_0} \right] \underbrace{\left[ \alpha \bar{\mathbf{K}}_{\Omega\Omega}^{-1} \bar{\mathbf{K}}_{\Omega\Gamma} \right]}_{\text{ALE mesh motion}} \underbrace{\frac{d\dot{\mathbf{x}}_{\Gamma}}{ds_i}}_{\text{SDESIG}} \right)$$

$$\alpha = \begin{cases} 1 & \text{in ALE framework} \\ 0 & \text{in Embedded framework} \end{cases}$$

## ANALYTIC DERIVATIVES

$$\frac{\partial \mathbf{R}}{\partial s_i}$$

- Approach
  - Separate treatment of inviscid and viscous contribution
  - Re-use information from the intersector, obtained by FIVER, whenever possible
- Inviscid part

$$\mathbf{R}_{ij}^{c,i} = \phi_{ij}^i(\tilde{\mathbf{w}}_{ij}, \tilde{\mathbf{w}}_{ij}^*(s), \mathbf{n}_{ij})$$
$$\frac{\partial \mathbf{R}_{ij}^{c,i}}{\partial s} = \frac{\partial \mathbf{R}_{ij}^{c,i}}{\partial \mathbf{w}_{ij}^*} \frac{\partial \mathbf{w}_{ij}^*}{\partial s}$$

## ANALYTIC DERIVATIVES

$$\frac{\partial \mathbf{R}}{\partial s_i}$$

- Diffusive part

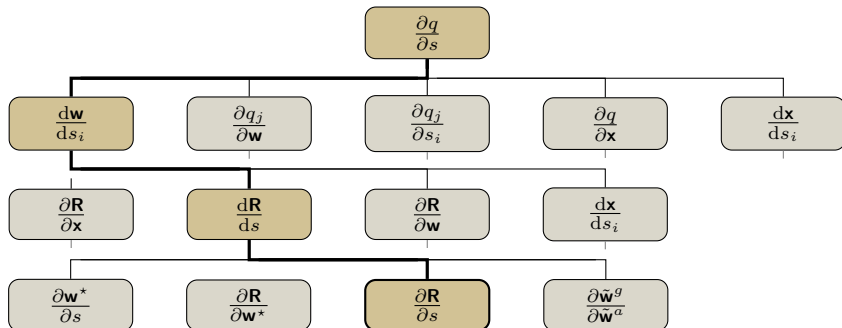
$$\mathbf{R}_i^v = - \sum_{T_i \in \lambda(i)} \sum_{i=1}^{n_g} w_i \tilde{\mathbb{K}} \nabla \tilde{\mathbf{w}}(\mathbf{x}_i) \nabla \phi_j(\mathbf{x}_i) dx$$

$$\frac{\partial \mathbf{R}^v(s, \tilde{\mathbf{w}}^a(s), \tilde{\mathbf{w}}^g(\tilde{\mathbf{w}}^a(s)), \mathbf{x}(s))}{\partial s} =$$

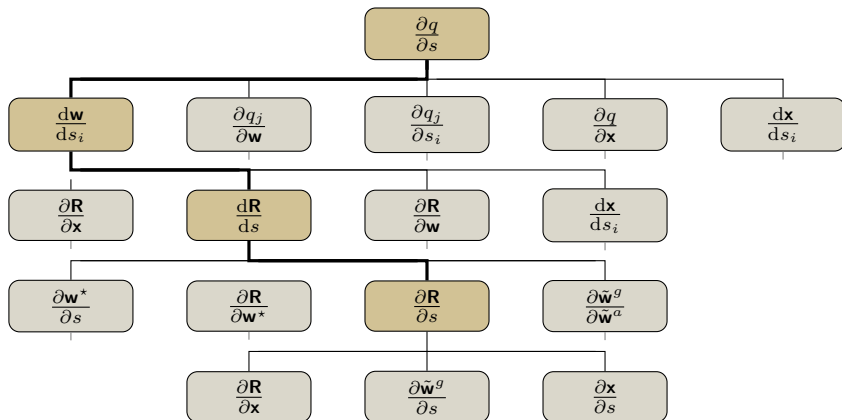
obtained during the  
population process

$$\underbrace{\frac{\partial \mathbf{R}^v}{\partial \tilde{\mathbf{w}}^a} \frac{\partial \tilde{\mathbf{w}}^a}{\partial s}}_{\substack{\text{can be re-used from ALE} \\ \text{after the ghost-point population}}} + \frac{\partial \mathbf{R}^v}{\partial \tilde{\mathbf{w}}^g} \cdot \underbrace{\frac{\partial \tilde{\mathbf{w}}^g}{\partial \tilde{\mathbf{w}}^a}}_{\text{obtained during the population process}} \frac{\partial \tilde{\mathbf{w}}^a}{\partial s} + \underbrace{\frac{\partial \mathbf{R}}{\partial \mathbf{x}} \frac{\partial \mathbf{x}}{\partial s}}_{=0 \text{ for embedded}}$$

## AAA



## AAA



## OUTLINE FOR SECTION 4

- 1 INTRODUCTION
- 2 AERODYNAMIC OPTIMIZATION
- 3 SENSITIVITY ANALYSIS
- 4 NUMERICAL FRAMEWORK**
- 5 NUMERICAL RESULTS
- 6 VERIFICATION

## COMPRESSIBLE NAVIER STOKES EQUATIONS

The compressible Navier Stokes equations in conservative form can be written as

$$\underbrace{\frac{\partial \bar{\mathbf{w}}}{\partial t}}_{\text{time derivative}} + \underbrace{\nabla \cdot \mathcal{F}(\bar{\mathbf{w}})}_{\text{inviscid}} + \underbrace{\nabla \cdot \mathcal{G}(\bar{\mathbf{w}})}_{\text{viscous}} = \underbrace{S(\bar{\mathbf{w}}, \chi_1, \dots, \chi_m)}_{\text{source term}}$$

Inviscid fluxes

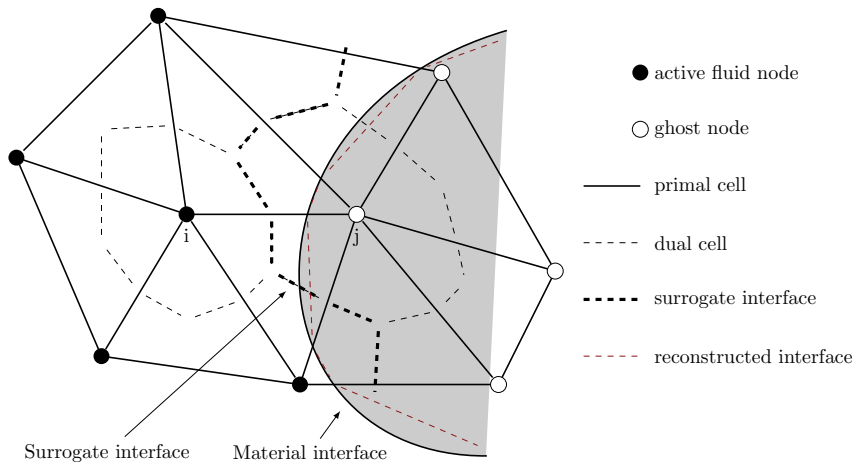
$$\mathcal{F} = \mathbf{w} \mathbf{v}^T + p \begin{bmatrix} 0 \\ \mathbf{I} \\ \mathbf{v}^T \end{bmatrix}$$

Viscous fluxes

$$\mathcal{G} = \begin{bmatrix} \mathbf{0} \\ \boldsymbol{\tau} \\ \boldsymbol{\tau} \mathbf{v} + \mathbf{q} \end{bmatrix}$$



## SETUP



## DISCRETIZATION

- Body-fitted and Immersed boundaries (FIVER)
- FE-like treatment of the viscus term

$$\frac{\partial \mathbf{w}_i}{\partial t} + \int_{\partial \mathcal{C}_i} \mathcal{F}(\mathbf{w}) \cdot dS - \int_{\Sigma_{T_i}} \mathbb{K} \mathbf{w} \nabla \phi_i dx = \mathbf{0}$$

$$\int_{\partial \mathcal{C}_i} \mathcal{F}(\mathbf{w}) \cdot dS \approx \underbrace{\sum_{j \in \kappa(i)^a} \phi_{ij}(\mathbf{w}_i, \mathbf{w}_j, \nu_{ij})}_{\text{non-intersected elements}} + \underbrace{\sum_{j \in \kappa(i) \setminus \kappa(i)^a} \phi_{ij}(\mathbf{w}_i, \mathbf{w}^*, \nu_{ij})}_{\text{intersected elements treated with FIVER}}$$

FIVER<sup>3</sup>  $\phi$  ... flux function of Roe<sup>4</sup>

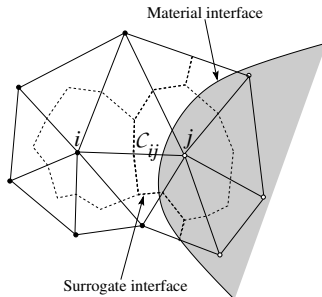
---

<sup>3</sup>Main2014.

<sup>4</sup>Roe1981.

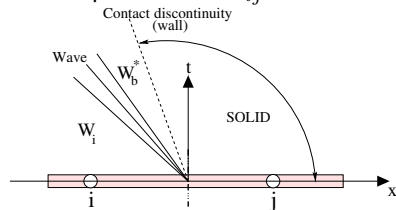
## IB WITH THE FIVER APPROACH: ORIGINAL FORMULATION

- Identify immersed boundaries with control volume interfaces  $\mathcal{C}_{ij}$



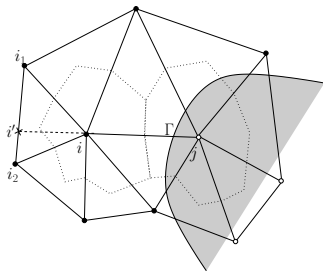
- Solve exactly local one-dimensional half-Riemann problems at  $\mathcal{C}_{ij}$

$$\begin{cases} \frac{\partial \tilde{\mathbf{w}}^*}{\partial \tau} + \frac{\partial \tilde{\mathbf{f}}(\tilde{\mathbf{w}}^*)}{\partial \xi} = 0 \\ \tilde{\mathbf{w}}^*(\xi, 0) = \tilde{\mathbf{w}}_{ij}, & \xi \leq 0 \\ \mathbf{v}(0, \tau) \cdot \mathbf{n}_{\text{wall}} = \mathbf{v}_{\text{wall}} \cdot \mathbf{n}_{\text{wall}}, & 0 \leq \tau \leq \Delta t \end{cases}$$



- Evaluate numerical flux:  $\mathbf{F}_{ij} = \mathbf{F}_{ij}(\mathbf{w}_{ij}, \mathbf{w}_b^*, \mathbf{n}_{ij})$

# IB WITH THE FIVER APPROACH: ENHANCED FORMULATION



- The fluid state is extrapolated to the material interface  $\Gamma$

$$\mathbf{w}_{\Gamma} = \mathbf{w}_i + \nabla \mathbf{w}_i \cdot (\mathbf{x}_{\Gamma} - \mathbf{x}_i)$$

- The one-dimensional half-Riemann problem is solved at material interface  $\Gamma$

$$\tilde{\mathbf{w}}_{\Gamma}^* = \tilde{\mathbf{w}}^*(\tilde{\mathbf{w}}_{\Gamma}, \mathbf{v}_{\text{wall}}, \mathbf{n}_{\text{wall}})$$

- The fluid state is inter/extrapolated at control volume interface  $\mathcal{C}_{ij}$

$$\mathbf{w}_{ij}^* = \mathbf{w}_{ij}^*(\mathbf{w}_{\Gamma}^*, \mathbf{w}_{i'})$$

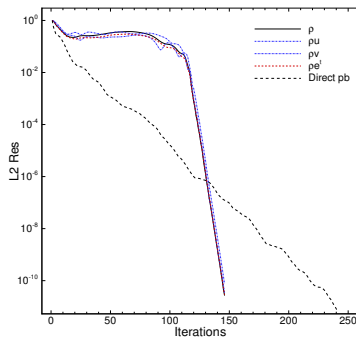
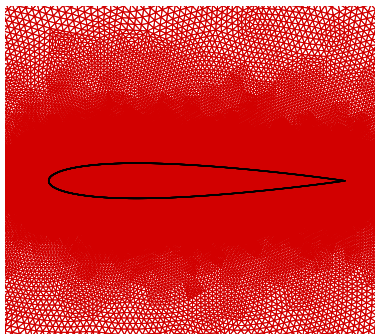
- Numerical flux at the control volume interface:  $\mathbf{F}_{ij} = \mathbf{F}_{ij}(\mathbf{w}_{ij}, \mathbf{w}_{ij}^*, \mathbf{n}_{ij})$
- Second-order convergence is recovered in the vicinity of the interface

## OUTLINE FOR SECTION 5

- 1 INTRODUCTION
- 2 AERODYNAMIC OPTIMIZATION
- 3 SENSITIVITY ANALYSIS
- 4 NUMERICAL FRAMEWORK
- 5 NUMERICAL RESULTS**
- 6 VERIFICATION

# VERIFICATION OF THE ANALYTICAL SENSITIVITIES

NACA-0012,  $Ma = 0.5$ ,  $\alpha = 2^\circ$



- 3D Grid  $\sim 200\,000$  nodes
- CFD CPU time  $\sim 10$  min
- Direct problem CPU time: seconds



## OUTLINE FOR SECTION 6

- 1 INTRODUCTION
- 2 AERODYNAMIC OPTIMIZATION
- 3 SENSITIVITY ANALYSIS
- 4 NUMERICAL FRAMEWORK
- 5 NUMERICAL RESULTS
- 6 VERIFICATION**

- Validating the fluid Jacobian via Finite Difference

$$\left. \frac{\partial \mathbf{R}}{\partial \mathbf{w}} \right|_{\mathbf{w}_0} \mathbf{u} = \frac{\mathbf{R}_i(\mathbf{w}_0 + \epsilon \mathbf{u}) - \mathbf{R}_i(\mathbf{w}_0 - \epsilon \mathbf{u})}{2\epsilon}$$

- Validate the fluid solution via the finite difference of two steady state simulations

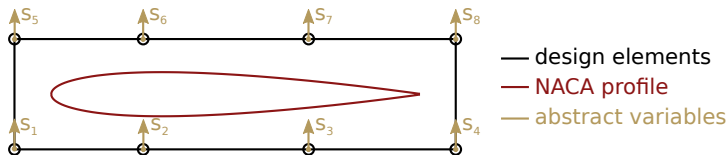
$$\left. \frac{d\mathbf{w}(s)}{ds} \right|_{w_0} = \frac{\mathbf{w}(s + \epsilon) - \mathbf{w}(s - \epsilon)}{2\epsilon}$$

- Validating both Body-fitted and Embedded formulation

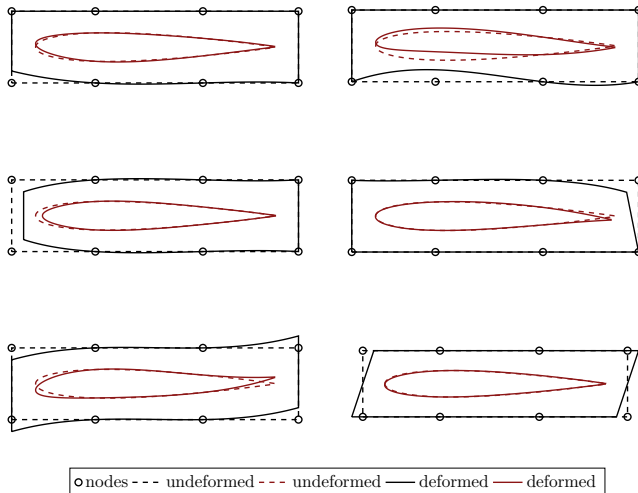


## Simple NACA0012 profile

- $\alpha = 0.0^\circ, 3.0, 6.0, 9.0$
- $M = 0.1, 0.3, 0.7, 0.9$
- Stiffened Gas



# SHAPE-MODIFICATION VIA DESIGN VARIABLES



# VERIFICATION OF $\frac{\partial \mathbf{w}}{\partial s}$ BODY-FITTED

**Verification  $\frac{d\mathbf{w}}{dM_\infty}$  for RANS equations and a body-fitted framework**

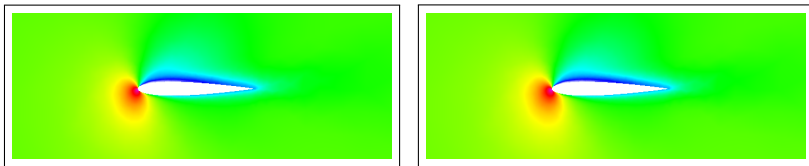


**FIGURE:**  $\frac{d\mathbf{w}_1}{dM_\infty}$ : FD-sensitivity on the left, analytic sensitivity

# VERIFICATION OF $\frac{\partial \mathbf{w}}{\partial s}$ BODY-FITTED

**Verification  $\frac{d\mathbf{w}}{dM_\infty}$  for RANS equations and a body-fitted framework**

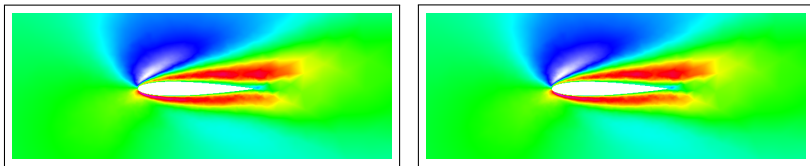


**FIGURE:**  $\frac{d\mathbf{w}_2}{dM_\infty}$ : FD-sensitivity on the left, analytic sensitivity

# VERIFICATION OF $\frac{\partial \mathbf{w}}{\partial s}$ BODY-FITTED

**Verification  $\frac{d\mathbf{w}}{dM_\infty}$  for RANS equations and a body-fitted framework**

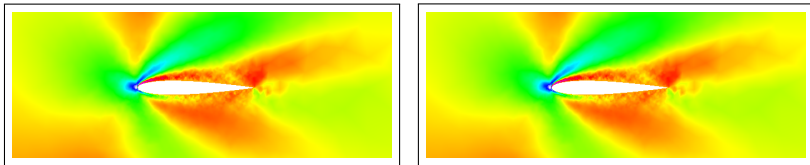


**FIGURE:**  $\frac{d\mathbf{w}_3}{dM_\infty}$ : FD-sensitivity on the left, analytic sensitivity

# VERIFICATION OF $\frac{\partial \mathbf{w}}{\partial s}$ BODY-FITTED

**Verification  $\frac{d\mathbf{w}}{dM_\infty}$  for RANS equations and a body-fitted framework**

# VERIFICATION OF $\frac{\partial \mathbf{w}}{\partial s}$ BODY-FITTED

**Verification  $\frac{d\mathbf{w}}{dM_\infty}$  for RANS equations and a body-fitted framework**

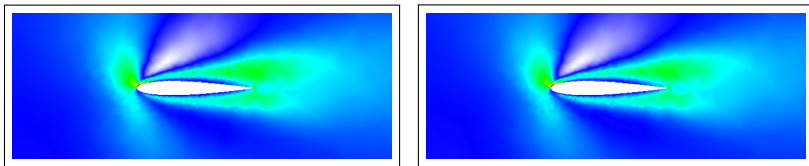


**FIGURE:**  $\frac{d\mathbf{w}_5}{dM_\infty}$ : FD-sensitivity on the left, analytic sensitivity

# VERIFICATION OF $\frac{\partial \mathbf{w}}{\partial s}$ BODY-FITTED

**Verification  $\frac{d\mathbf{w}}{dM_\infty}$  for RANS equations and a body-fitted framework**

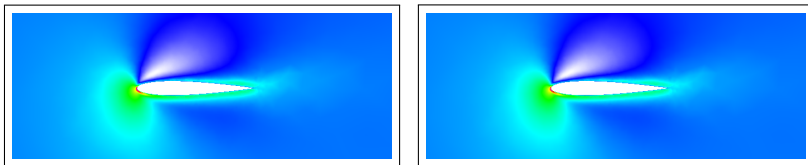


**FIGURE:**  $\frac{d\mathbf{w}_6}{dM_\infty}$ : FD-sensitivity on the left, analytic sensitivity



# VERIFICATION OF $\frac{\partial \mathbf{w}}{\partial s}$ EMBEDDED

**Verification  $\frac{dw}{dM_\infty}$  for RANS equations and an embedded framework**

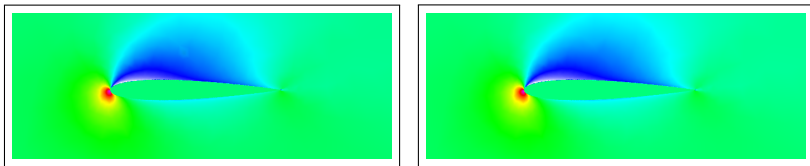


**FIGURE:**  $\frac{dw_1}{dM_\infty}$ : FD-sensitivity on the left, analytic sensitivity

# VERIFICATION OF $\frac{\partial \mathbf{w}}{\partial s}$ EMBEDDED

**Verification  $\frac{dw}{dM_\infty}$  for RANS equations and an embedded framework**

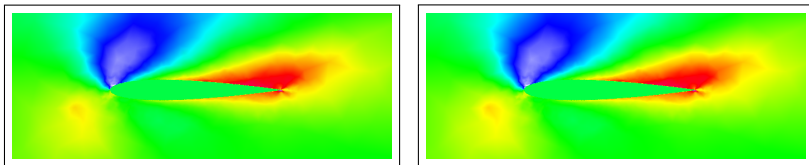


**FIGURE:**  $\frac{dw_2}{dM_\infty}$ : FD-sensitivity on the left, analytic sensitivity

# VERIFICATION OF $\frac{\partial \mathbf{w}}{\partial s}$ EMBEDDED

**Verification  $\frac{dw}{dM_\infty}$  for RANS equations and an embedded framework**

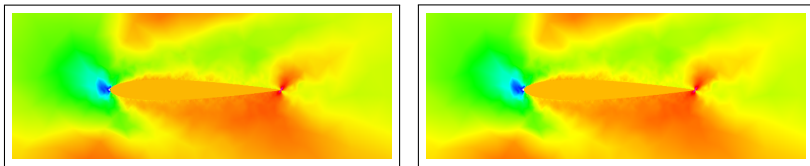


**FIGURE:**  $\frac{dw_3}{dM_\infty}$ : FD-sensitivity on the left, analytic sensitivity

# VERIFICATION OF $\frac{\partial \mathbf{w}}{\partial s}$ EMBEDDED

**Verification  $\frac{d\mathbf{w}}{dM_\infty}$  for RANS equations and a embedded framework**

# VERIFICATION OF $\frac{\partial \mathbf{w}}{\partial s}$ EMBEDDED

**Verification  $\frac{dw}{dM_\infty}$  for RANS equations and an embedded framework**

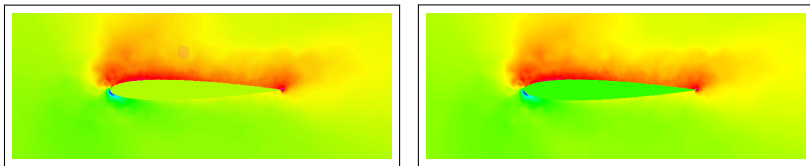


**FIGURE:**  $\frac{dw_5}{dM_\infty}$ : FD-sensitivity on the left, analytic sensitivity

# VERIFICATION OF $\frac{\partial \mathbf{w}}{\partial s}$ EMBEDDED

**Verification  $\frac{dw}{dM_\infty}$  for RANS equations and an embedded framework**

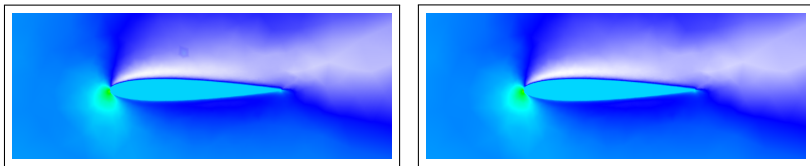


**FIGURE:**  $\frac{dw_6}{dM_\infty}$ : FD-sensitivity on the left, analytic sensitivity

## CONVERGENCE OF FORCE-SENSITIVITIES

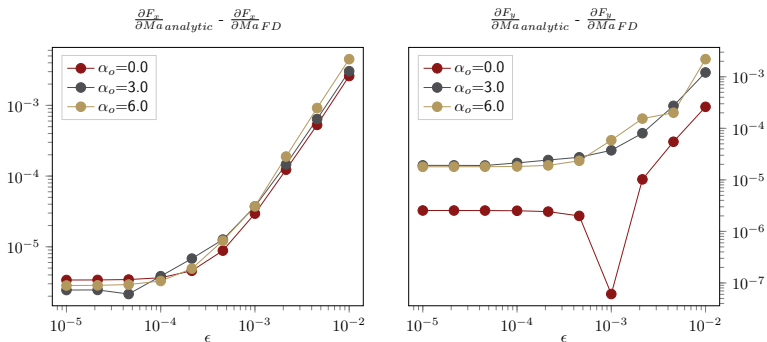
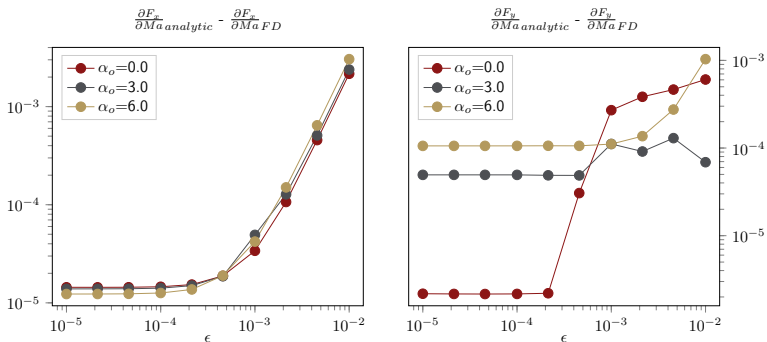


FIGURE: Convergence of the analytic results for Euler-equations

# CONVERGENCE OF FORCE-SENSITIVITIES



**FIGURE:** Convergence of the analytic results for Laminar-equations



## CONVERGENCE OF FORCE-SENSITIVITIES

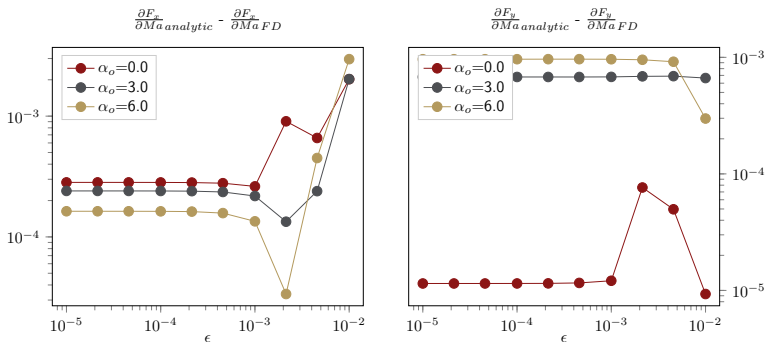


FIGURE: Convergence of the analytic results for RANS-equations

